Schizophrenia Bulletin vol. 46 no. 4 pp. 990–998, 2020
doi:10.1093/schbul/sbz129
Advance Access publication 28 January 2020

Miswiring of Frontostriatal Projections in Schizophrenia

James J. Levitt*[,1,2], Paul G. Nestor[1,3], Marek Kubicki[2,4,5], Amanda E. Lyall[2,5], Fan Zhang[4], Tammy Riklin-Raviv[6], Lauren J. O'Donnell[4], Robert W. McCarley[1,†] Martha E. Shenton[2,4,5,7], and Yogesh Rathi[2,5]

[1]Clinical Neuroscience Division, Laboratory of Neuroscience, Department of Psychiatry, VA Boston Healthcare System, Brockton Division, Brockton, MA, Harvard Medical School, Boston, MA; [2]Psychiatry Neuroimaging Laboratory, Department of Psychiatry, Brigham and Women's Hospital, Harvard Medical School, Boston, MA; [3]Department of Psychology, University of Massachusetts, Boston, MA; [4]Department of Radiology, Brigham and Women's Hospital, Harvard Medical School, Boston, MA; [5]Department of Psychiatry, Massachusetts General Hospital, Harvard Medical School, Boston, MA; [6]Department of Electrical and Computer Engineering, Ben Gurion University, Beer-Sheva, Israel; [7]VA Boston Healthcare System, Brockton Division, Brockton, MA

[†]Deceased.
*To whom correspondence should be addressed; Department of Psychiatry-116A, VA Boston Healthcare System, Harvard Medical School, 940 Belmont Street, Brockton, MA 02301; tel: (508) 583-4500 x61798, fax: 617-525-6150, e-mail: james_levitt@hms.harvard.edu

We investigated brain wiring in chronic schizophrenia and healthy controls in frontostriatal circuits using diffusion magnetic resonance imaging tractography in a novel way.We extracted diffusion streamlines in 27 chronic schizophrenia and 26 healthy controls connecting 4 frontal subregions to the striatum. We labeled the projection zone striatal surface voxels into 2 subtypes: dominant-input from a single cortical subregion, and, functionally integrative, with mixed-input from diverse cortical subregions.We showed: 1) a group difference for total striatal surface voxel number ($P = .045$) driven by fewer mixed-input voxels in the left ($P = .007$), but not right, hemisphere; 2) a group by hemisphere interaction for the ratio quotient between voxel subtypes ($P = .04$) with a left ($P = .006$), but not right, hemisphere increase in schizophrenia, also reflecting fewer mixed-input voxels; and 3) fewer mixed-input voxel counts in schizophrenia ($P = .045$) driven by differences in left hemisphere limbic ($P = .007$) and associative ($P = .01$), but not sensorimotor, striatum.These results demonstrate a less integrative pattern of frontostriatal structural connectivity in chronic schizophrenia. A diminished integrative pattern yields a less complex input pattern to the striatum from the cortex with less circuit integration at the level of the striatum. Further, as brain wiring occurs during early development, aberrant brain wiring could serve as a developmental biomarker for schizophrenia.

Key words: schizophrenia/diffusion magnetic resonance imaging/tractography/brain wiring/striatum/prefrontal cortex

Introduction

The cortical-subcortical basal ganglia network, which contains the frontostriatal circuits, is of interest in neuropsychiatric conditions such as schizophrenia because its subcortical thalamic output targets cognitive and limbic regions in the prefrontal cortex as well as motor regions in the frontal cortex. This allows the basal ganglia to modulate non-motor, cognitive, and emotional functions in addition to motor function.[1–3] Functional areas of the cortex project in a generally topographic manner to the striatum which, consequently, has been divided into three functional zones: limbic, associative, and sensorimotor based on receiving projections from corresponding cortical functional areas. These topographic projections have been described as forming three spatially and functionally segregated corticostriatal-thalamic feedback subloops.[4] Abnormalities in the corticostriatal projections in any of the three subloops could disrupt the functioning of the entire subloop and adversely affect cognitive, affective, or sensorimotor function.[5–10]

Cortical axonal projections to the striatum, however, are not exclusively topographically arranged (eg, [11–13]). Different striatal projection zones receive either overlapping, ie, mixed-input, from anatomically and functionally diverse cortical subregions (integrative zones) or dominant-input from a single anatomical and functional cortical subregion (segregated zones) (see figure 1). The presence of such integrative and segregated corticostriatal target zones is strongly supported by both animal tract tracing and human imaging studies.[11,12,14,15] Striatal target zones that receive overlapping cortical projections allow

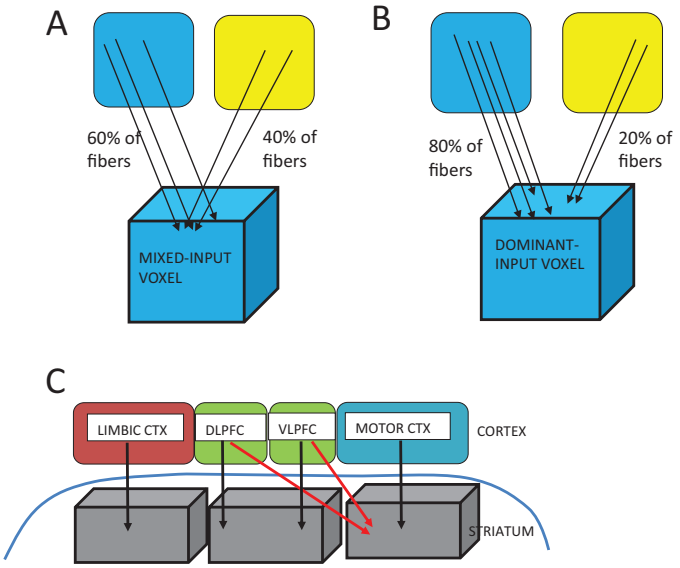

Fig. 1. **A.** Mixed-input voxel (<0.7 threshold; left and right blue and yellow boxes represent different cortical functional subregions). **B.** Dominant-input voxel (>0.70% threshold; left and right blue and yellow boxes represent different cortical functional subregions). **C.** Model of frontostriatal connections. Parallel, segregated streamlines (4 black arrows) are shown, as well as convergent, integrative streamlines (2 red arrows). Far right voxel is representative of an overlapping-input striatal surface voxel; left and middle voxels are representative of dominant-input voxels. CTX: Cortex; DLPFC: dorsolateral prefrontal cortex; VLPFC: ventrolateral prefrontal cortex.

for the integration of information from different cortical functional subregions (eg, [12,13]).

Such an anatomic organization of frontostriatal connectivity would result in different local connectivity patterns on the surface of the striatum. Based on frontostriatal streamline counts, using dMRI tractography, we used diffusion MRI (dMRI) tractography in a novel way to detect such local variation by describing the degree of overlap in the projection zones of the outflow of streamlines from frontal cortex to the striatum. Based on the degree of such overlap, we labeled striatal surface voxels into 2 types: 1) segregated, or dominant voxels, (receiving dominant-input from a single functional cortical area); and, 2) integrative, or mixed voxels, (receiving mixed-input from diverse functional cortical areas). Second, to assess the balance between dominant and mixed voxels, we calculated what we termed a voxel type ratio (VTR) quotient which reflects the relative amount of segregated (dominant-input) vs integrative (mixed-input) striatal surface voxels in each hemisphere. The novelty of this dMRI approach is its focus on the projection zone pattern on the striatal surface rather than on diffusion measures of the axonal projections, themselves.

Previously, we showed reduced striatal connectivity in both first-episode and chronic schizophrenia in frontostriatal tracts using the diffusion measures of fractional anisotropy (FA) and mean diffusivity (MD).[10,16] To extend our earlier analyses of the microstructural diffusion properties of the frontostriatal white matter tracts, here, we assess group differences in brain wiring in this circuit. We hypothesize a less integrative projection zone pattern on the striatal surface in schizophrenia. More specifically, we predict 1) fewer number of mixed-input striatal surface voxels in schizophrenia; 2) a larger VTR quotient in schizophrenia driven by fewer mixed-input voxels; and 3) group differences in the number of mixed-input voxels in limbic and associative striatal subregions, which subserve emotional and cognitive function, but not in the sensorimotor subregion.

Methods

Subjects

Twenty-seven male patients diagnosed with chronic schizophrenia were recruited from the VA Boston Healthcare System in Brockton, MA. Assessments with the Structured Clinical Interview for DSM-IV-Patient Version (SCID)[17] were used to make DSM-IV diagnoses. The non-patient edition of the SCID[18] was completed for 26 males, healthy control subjects who were recruited from the general community and were group matched on age, sex, handedness,[19] and parental socioeconomic status[20] to the patient sample. Subject inclusion criteria were: right-handedness, 17 to 55 years of age, no history of electroconvulsive shock treatment, no history of neurological illness, no alcohol or drug abuse in the last 5 years, no medication with known effects on MR (such as steroids), and a verbal IQ above 75. Additionally, healthy controls were screened to exclude individuals who have a first-degree relative with an Axis I disorder. Written informed consent was obtained from all subjects after they received a complete description of the study. IRB approval for this study was approved by the local IRB committees at the VA Boston Healthcare System and at the Brigham and Women's Hospital.

Image Acquisition and Preprocessing. For structural and DWI measurements, images were acquired using a 3 Tesla whole body General Electric MRI scanner (GE Medical Systems, Milwaukee) with a voxel size of 1 × 1 × 1 mm. The MRI sequences included a high resolution 3D T1 (IR-FSPGR, TR 7.79 ms, TE 2.98 ms, TI 600 ms, flip angle 10°, FOV matrix size 256 × 256, 176 slices, 1-mm slice thickness). Diffusion-weighted images were acquired using a twice-refocused echo-planar imaging sequence (TR 17 s, TE 80 ms, flip angle 90°, FOV matrix size 144 × 144, 85 slices, 1.7-mm slice thickness, 51 gradient directions with b = 900 s/mm^2 and eight baseline scans with b = 0).

Preprocessing was performed using our laboratory's standard pipeline that includes motion correction and manual brain masking.

Structural Image Post-Processing. All regions of interests (ROIs) were obtained from structural MRIs and then

registered to the diffusion MRI images. Cortical ROIs were automatically parcellated using the FreeSurfer, and the whole striatum ROI was segmented using manual tracing. Using the FreeSurfer software package (version 4.0.2), we parcellated T1-weighted Spoiled Gradient Echo (SPGR) images into cortical gray and white matter regions for each subject.[21] We also acquired high resolution 3D T2W images (TR of 3 s, a TE of 90 ms, a 90° flip angle, a FOV of 256 × 256mm, a matrix size of 256 × 256, 176 slices, and 1-mm slice thickness). Using the FSL's nonlinear image registration tool (FNIRT) algorithm in the FSL software,[22] the T2 image for the same subject in the same coordinate space as the SPGR image was then registered to the baseline diffusion-weighted image. Whereas FreeSurfer software was used to parcellate cortical regions of interest,[21] the more difficult to delineate subcortical striatal regions of interests, both whole and subdivided striatum, were parcellated manually based on our published manual parcellation approach, with excellent reliability,[8,23] using the image-editing tool, *3D-Slicer*, (http://www.slicer.org). The person who traced the striatum was blind to subjects' demographics. Specifically, we defined the limbic striatum (LST) as the ventral striatum, the associative striatum (AST) as including the pre- and post-commissural caudate and pre-commissural putamen, and the sensorimotor striatum (SMST) as the post-commissural putamen for which reliability has previously been established.[10,23,24] See the Supplementary section and supplementary figure S1 for details of this tracing methodology, including our method to delineate an oblique line that separates the ventral striatum from the the caudate and putamen, the dorsal striatum, and for separating the striatum into 3 functional subregions, ie, the LST, AST, and SMST.

Diffusion Imaging Two-Tensor Whole Brain Tractography Post-Processing. We corrected for head motion, with an in-house script utilizing the FSL software framework[25] to spatially register (rigid registration) each of the diffusion-weighted images to the first non-diffusion-weighted (b = 0) image and subsequently updated the corresponding gradient directions to account for head motion (https://github.com/pnlbwh). Further, we conducted a statistical test with the motion parameters obtained for both groups and found no significant difference between the head motion parameters.[26] We, therefore, believe that motion is unlikely to be a contributor to the group differences observed in the analyses. We used the Unscented Kalman Filter (UKF) based two-tensor tractography algorithm[27] to trace fiber paths throughout the whole brain.[27,28] We seeded all voxels where the single-tensor FA was greater than 0.18. To generate streamlines, voxels were randomly seeded 10 times and each generated streamline was traced from seed to termination.

The multi-tensor tractography algorithm[27] used in this work was judged as one of the best tractography algorithms in a "Fiber Cup" challenge held during MICCAI 2009.[29] It allows to faithfully trace fibers through crossing regions while estimating the tensor parameters in a consistent manner. The generated tracts were manually inspected to ensure that the fibers enter into the cortical and subcortical gray matter regions. The termination criterion, we employed based on these tests, was, thus, set to FA < 0.15 for the primary tensor as described in detail by Malcolm et al.[27]

Calculating Ratio of Striatal Surface Areas (RSA) Based on Cortical Connectivity. We used FreeSurfer to select 4 frontal cortical ROIs as our cortical seed regions: 1) limbic cortex (comprised of rostral anterior cingulate gyrus and medial and lateral orbitofrontal cortex); 2) dorsolateral association prefrontal cortex (DLPFC; comprised of rostral middle frontal gyrus); 3) ventrolateral association prefrontal cortex (VLPFC; comprised of inferior frontal gyrus); and 4) motor cortex (comprised of caudal middle frontal gyrus and precentral gyrus) (see figure 2). We selected the manually traced whole striatum as our target region. We extracted streamlines derived from the whole brain UKF tractography that connected each frontal cortical ROI with the striatum. Based on its connectivity profile with the above 4 frontal cortical ROIs, we labeled each surface voxel of the striatum. We used a threshold proportion of 0.7 such that if a given surface voxel received more than 0.7 of its streamline counts from a given cortical seed region, it was labeled as a dominant (segregated) voxel corresponding to that seed region (ie, a majority, more than 70%, of the input streamlines to this voxel were from a single functional

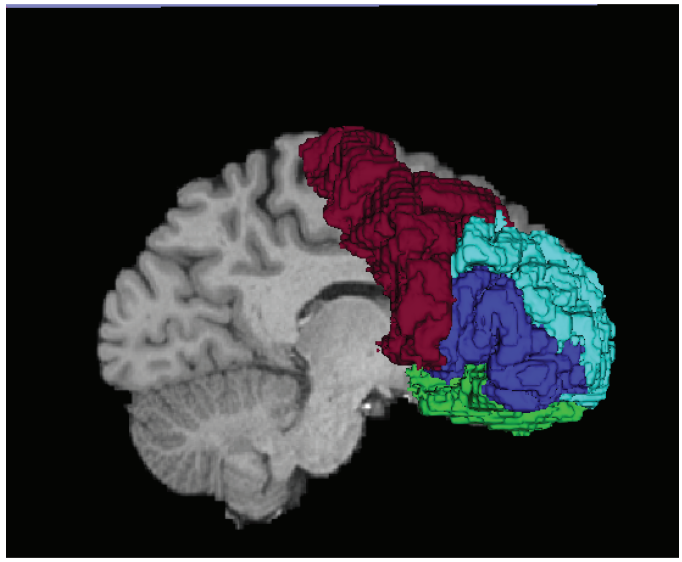

Fig. 2. 3D rendering of FreeSurfer frontal cortical ROIs. DLPFC is light blue; VLPFC is dark blue; Motor cortex is Red; Limbic cortex (rACG & OFC) is green. Only OFC is shown. DLPFC: dorsolateral prefrontal cortex; VLPFC: ventrolateral prefrontal cortex; rACG: rostral anterior cingulate gyrus; OFC: orbitofrontal cortex.

cortical subregion). If not, it was labeled as a mixed (integrative) voxel (see figure 1). We, thus, obtained 5 surface voxel subtypes (4 dominant subtypes based on receiving dominant-input from either DLPFC, VLPFC, limbic, or motor subregions, and 1 mixed subtype which did not receive dominant-input from any specific cortical functional subregion). We calculated surface subtype voxel counts, bilaterally, for both the whole striatum and for each striatal functional subregion (ie, LST, AST, and SMST; see supplementary figure S1).

To test for a group difference in the relative amount of striatal surface area receiving dominant-input vs mixed-input, we calculated a VTR quotient. This represents the relative ratio of striatal surface area voxels receiving dominant-input versus mixed-input from the cortex; ie, the proportion of the 2 types of cortical projection zone patterns on the striatal surface.

Specifically, we calculated the VTR quotient separately for the left hemisphere (LH) and the right hemisphere (RH) striatum, using the following formula: (LH dominant-input voxels − LH mixed-input voxels) / (LH dominant-input voxels + LH mixed-input voxels) × 0.5; (RH dominant-input voxels − RH mixed-input voxels) / (RH segregated voxels + RH mixed-input voxels) ×0.5.

Statistical Analysis

To test for group differences, mixed-model ANOVAs for number of all surface voxel subtypes, VTR quotients and for number of mixed voxels, alone, were used. A mixed-model ANOVA was used with diagnostic group as the "between-subjects" factor, hemisphere (left, right), and surface voxel subtype type (DLPFC, VLPFC, limbic, motor, mixed), as the "within-subjects" factors, for total surface subtype voxel number. A follow-up mixed-model ANOVA was used with diagnostic group as the "between-subjects" factor, hemisphere (left, right) and striatal functional region (LST, AST, SMST), as the "within-subjects" factors, for surface mixed voxel number. A mixed-model ANOVA was used with diagnostic group as the "between-subjects" factor, and hemisphere (left, right) as the "within-subjects" factor, for total striatal VTR quotient. Striatal surface voxel counts and striatal VTR quotients were the dependent measures used, respectively, in these models. In the case of a significant main effect or interaction, *post hoc t*-tests were used with significance set at $P < .05$ (two-tailed) to compare group mean differences, separately for LH and RH. We used the false-discovery rate correction for multiple comparisons.

Results

Subject Demographics

Mean age did not differ between schizophrenia and healthy controls (44.19 ± 11.1 vs 39.65 ± 11.10, $P = .118$). Parental socioeconomic status also showed no significant difference between groups ($P = .27$). As anticipated, however, there were significant differences in verbal IQ (98.6 ± 13.63, $n = 27$, vs 112.78 ± 16.26, $n = 18$, $P = .002$) and subject socioeconomic status (3.37 ± 1.08, $n = 27$, vs 1.94 ± 0.80, $n = 24$, $P < .001$). Used as a proxy measure of premorbid IQ, the Wide Range Achievement Test Reading Score (WRAT-RS) did not significantly differ between the 2 groups (98.26 ± 12.29, $n = 25$ vs 104.50 ± 10.2, $n = 16$, $P = .09$). Patients received a mixture of typical and atypical neuroleptic medications and were taking a mean dosage of 417.35 + 325.29 chlorpromazine mg equivalents, based on the conversion table of Stoll[30] for typical neuroleptics and the conversion table of Woods[31] for atypical neuroleptics. The schizophrenia patients had a mean age of onset of 23.83 ± 5.79 ($n = 23$) and a mean duration of illness of 20.22 years ± 10.22 ($n = 23$). The clinical Positive and Negative Syndrome Scale (PANSS; [32]) scores as well as demographic and medication information are included in table 1.

Measures of Striatal Surface Voxel Type and Surface Pattern

To test for a group difference in whole striatum surface voxel subtype counts, a mixed-model ANOVA was performed with group as the "between-subjects" factor, and side (left, right) and voxel subtype (limbic, dorsolateral PFC associative, ventrolateral PFC associative, motor, mixed) as the "within-subjects" factors. Results showed a main effect for group for surface voxel number ($F(1,51) = 4.2$, $P = .045$). We did not find any significant group by surface voxel-type interactions. *Post hoc t*-tests showed fewer mixed voxels in the LH but not in the RH ($P = .007$; $P = .2$), in chronic schizophrenia subjects compared with healthy controls (see figure 3, Panel A). However, when we corrected with a false-discovery rate *P*-value criterion of .05, none of the *post hoc t*-tests were significant.

Additionally, to test for a group difference in the input pattern of striatal surface area, we reduced our surface voxel subtypes from 5 to 2 subtypes: 1) non-mixed voxels, which we created by combining all non-mixed voxel subtypes into a single non-mixed voxel category and 2) mixed voxels. We then calculated a VTR quotient (equation shown in the Methods section) which provided a relative ratio between the number of non-mixed and mixed voxels on the surface of the striatum. To test for group differences in VTR quotients, a mixed-model ANOVA was performed with group as the "between-subjects" factor, and side (left, right) and VTR quotient as the "within-subjects" factor. Results showed a main effect for side ($P < .04$), a trend effect for group ($P = .06$) and, of note, a significant group by hemisphere interaction ($P = .04$). *Post hoc t*-tests showed a left, but not right, hemisphere increase in VTR quotient in schizophrenia vs healthy controls ($P = .006$; $P = .5$; figure 3, Panel B). Applying a false-discovery rate *P*-value criterion of .05, the LH VTR group difference remained statistically significant.

Table 1. Demographic, Neuropsychological, and Clinical measures

	Male schizophrenia subjects (n = 27)		Male healthy control subjects (n = 26)				
	Mean	SD	Mean	SD	*df*	*t*-test	*P*-value
Age (years)	44.19	9.62	39.65	11.10	1, 51	−1.59	.118
Handedness[b]	0.72 (n = 27)	0.24	0.79 (n = 26)	0.17	1, 51	1.250	.217
Socioeconomic status[c]							
Subjects's own	3.37 (n = 27)	1.08	**2.22** (n = 24)	0.**81**	1, **47.7**	−5.0**1**	<.001**
Parental	2.5**9** (n = 26)	1.1**4**	2.22 (n = 23)	**1.13**	1, **47**	−1.**11**	.**27**
WAIS-III Verbal IQ	98.26 (n = 27)	13.63	112.78 (n = 18)	16.26	1, 43	3.24	.002**
WRAT3_RS[d]	98.08 (n = 25)	12.29	104.50 (n = 16)	10.22	1, 39	1.76	.090
Symptom onset (age)	**23.83 (n = 23)**	**±5.79**	**NA**				
Duration of illness (years)	**20.22 (n = 23)**	**±10.22**	**NA**				
Antipsychotic Medication Dosage[e]	417.35	325.29	NA				
PANSS (Sum of Positive Scores)	20.65 (n = 26)	8.80	NA				
PANSS (Sum of Negative Scores)	20.54 (n = 26)	9.83	NA				
PANSS (Sum of General Scores)	41.15 (n = 26)	16.47	NA				
PANNS (Sum of all PANSS Scores)	82.35 (n = 26)	28.05	NA				

Note: WAIS-III = Wechsler Adult Intelligence Scale—3rd Edition; SAPS = Scale for Assessment of Positive Symptoms; SANS = Scale for Assessment of Negative Symptoms; NA = data not applicable.
[a]The *df* differs among variables owing to unavailability of data in some participants. [b]Handedness was evaluated using the Edinburgh inventory and right -handedness is above zero. [c]Higher scores indicated lower socioeconomic status (Hollingshead, 1965). [d]Wide Range Achievement Test Reading Score (WRAT-RS). [e]Chorpromazine mg equivalents. Patients were receiving a mixture of typical and atypical medications; one patient was not taking medication at the time of the testing and three patients-specific medications were unknown.
**P < .01.

As both of our above results pointed to group differences being driven by reduced striatal surface mixed-input voxel counts, and as our original hypothesis was that chronic schizophrenia subjects would have a less integrative frontostriatal structural connectivity pattern as manifested by fewer striatal surface mixed voxels, we further examined the surface mixed-input voxels, alone.

Using a subregional analysis, we calculated the number of surface mixed-input voxels in each separate striatal functional subregion to determine where in the striatum the number of surface mixed-input voxels differed between groups. To test for group regional differences in striatal surface mixed-input voxel counts, a mixed-model ANOVA was performed with group as the "between-subjects" factor, and hemisphere (left, right) and striatal functional subregion (LST, AST, SMST), as the "within-subjects" factors. Results showed a main effect for group for striatal subregional mixed-input voxel counts ($F(1,51) = 4.0$, $P = .05$). We did not find a group by striatal subregion or any other interactions. *Post hoc t*-tests showed that the surface mixed-input voxel counts in the LH LST ($t = 2.8$, df = 51, $P = .007$) and LH AST ($t = 2.6$, df = 51, $P = .013$) were reduced in chronic schizophrenia compared with healthy controls. Applying the false-discovery rate correction for multiple comparisons, with a false-discovery rate *P*-value criterion of .05, we found that both LH LST and LH AST group differences remained statistically significant.

The Use of Multiple Thresholds to Test Threshold Validity in Calculating Striatal Surface Voxel Subtypes

To test the validity of our 0.7 threshold, we recalculated our results using 0.5 and 0.9 thresholds. We found similar results for both hemispheres; namely, that as the threshold increased, non-mixed voxel counts diminished and mixed voxels counts increased in smooth curves, with chronic schizophrenia subjects showing fewer mixed voxels for all thresholds. Thus, the use of different thresholds did not alter our results (see supplementary figure S2).

Discussion

The principal finding in this study is that chronic schizophrenia subjects have abnormal frontostriatal brain wiring compared to healthy controls due to a less integrative frontal projection zone pattern on the striatal surface. This, in turn, allows for less "cross-talk" between functionally diverse cortical areas in chronic schizophrenia at the level of the striatum. Specifically, first, we find that chronic schizophrenia subjects have fewer total striatal surface voxels labeled by cortical connectivity. This was driven by a reduction in number of mixed voxels in the LH striatum. Second, we find that chronic schizophrenia patients have a higher VTR quotient, ie, a higher ratio of dominant to mixed voxels, also consequent to fewer mixed voxels. Third, and lastly, we find that the overall

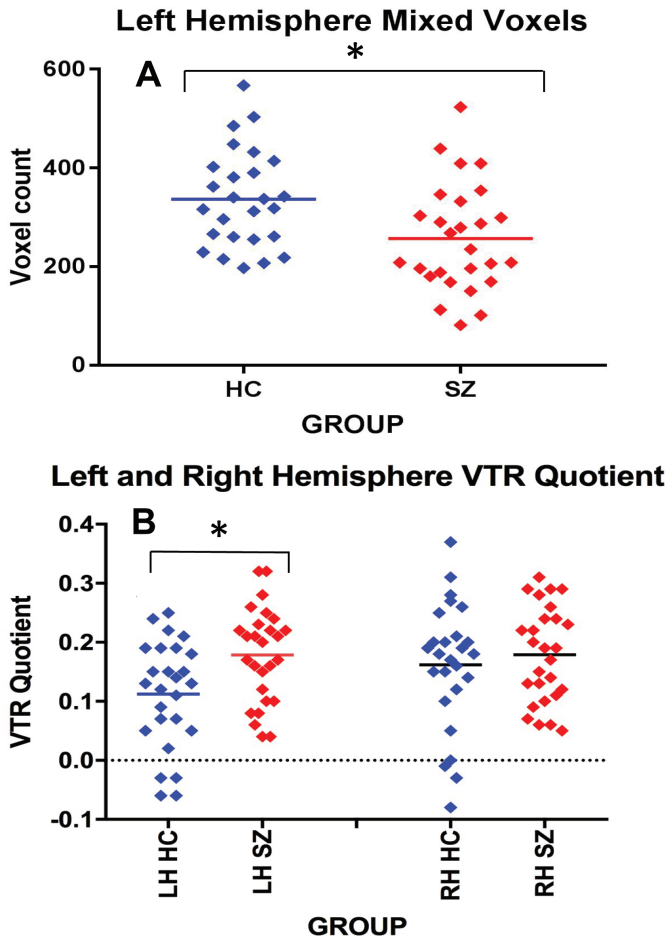

Fig. 3. **Panel A** scatter plot shows fewer mixed voxels in the left hemisphere on striatal surface in CSZ vs HCs. **Panel B** scatter plot shows an interaction between hemisphere and group; follow-up *t*-test shows larger VTR quotient in the LH in SZ vs HCs. * < .05. VTR (voxel type ratio).

reduction in mixed voxels in chronic schizophrenia was driven by a group difference in the LH limbic and associative, but not sensorimotor, striatum.

Understanding the pattern of axonal outflow from the frontal cortex to the striatum is important because it illuminates the impact of the basal ganglia on cortical function. The anatomic organization of corticostriatal connectivity has been extensively explored in animal tract tracing studies and more recently in *in vivo* brain imaging studies (eg, [33,34]). For example, Averbeck et al,[11] using animal tract tracing, found that certain projection zones of the striatum received inputs from all prefrontal regions which they examined, thus, allowing these target areas to serve as hubs for integrating information from diverse cortical functional subregions. Although our data do not indicate where fibers terminate in the striatum, the mixed voxels on the surface of the striatum similarly reflect a wiring pattern of convergence of outflow from diverse functional cortical subregions. Convergent with this, in healthy human subjects, Draganski et al,[14] using probabilistic diffusion imaging, also found overlap in the striatal projection zones of prefrontal, premotor, and motor cortex.

As brain wiring occurs during development, MRI measures of aberrant brain wiring could, thus, serve as biological markers for abnormal development. Such markers, for example, could identify early psychosis patients with abnormal development who might benefit from early intervention to protect against biological or social "second hit" stressors. Our results of aberrant brain wiring in adult schizophrenia support a developmental hypothesis of schizophrenia,[35,36] an idea strengthened by findings in genome-wide association studies (GWAS) which have identified developmental genes associated with SZ that affect neurogenesis, neuronal maturation, migration, and synaptic pruning.[37–39]

Our results are consistent with other studies that have utilized structural neuroimaging-based measures to assess macrostructural neurodevelopmental pathologies in schizophrenia. For instance, abnormal cortical brain folding has been reported in schizophrenia using measures of cortical surface area complexity (eg, [40]) and gyral index (eg, [41,42]). Further, and as noted in a review by White (2010), there are strong indications that link brain white matter connectivity to cortical gyrification.[43] White matter axonal tension may explain such a relationship.[44]

Additional support favoring abnormal neurodevelopment in disorders such as schizophrenia include that sulcal gyral patterns differ between groups.[45] For example, Yücel et al[46] showed that the frequency of the presence of the paracingulate sulcus, which forms a parallel sulcus to the anterior cingulate sulcus, differed between schizophrenia and healthy controls. Also, Nakamura et al[47] showed a difference between schizophrenia subjects and healthy controls in the configuration of the "H-shaped" sulcus in the orbitofrontal cortex. Cortical malformations in this region, which targets the limbic striatum,[48] might adversely affect the pattern of connectivity to the striatum with functional consequences. Of note, in our results, it is the limbic and associative striatum, but not sensorimotor striatum, in the LH, that show the largest reductions in the number of mixed voxels in schizophrenia.

In addition, our findings of more pronounced reductions in mixed-input voxels in limbic and associative vs sensorimotor subregions of the striatum are consistent with clinical presentations of schizophrenia characterized by greater deficits in emotion and cognition than in motor function. That our findings for mixed-input voxels were lateralized to the LH is consistent with the studies of asymmetry in schizophrenia.[49,50] One such study by Cullen et al,[51] eg, showed that in schizophrenia, compared to in healthy controls, there was a loss of left > right hemisphere cell density asymmetry which was secondary to lesser cell density and smaller soma in the LH dorsolateral prefrontal cortex.

Limitations of the study include the potential confound of neuroleptic medication on our white matter measures and the potential confound of chronicity. However, as the measures we use rely heavily on the proportion of streamline inputs from multiple cortical source ROIs to the striatal surface voxels, the impact of systemically used medication on our measures is mitigated by the fact that all the white matter streamlines from the different cortical source ROIs are similarly affected. Nevertheless, we believe that studies should be performed in prodromal and early psychosis schizophrenia patients to diminish the impact of the confounding effects of medication and chronicity of illness. An additional potential limitation in our study is that some data for subject demographic measures, as shown in table 1, are missing.

A further potential limitation is that our use of 0.7 as a threshold for the boundary between dominant and mixed voxels could be considered somewhat arbitrary and without a biological justification. We note, however, there is ample support in the literature for corticostriatal projection zone overlap (ie, what we would label as mixed voxels) in the striatum. The anatomic organization of corticostriatal connectivity has been extensively explored in monkey animal tract tracing studies. For example, Yeterian and Van Hoesen[52] found that reciprocally connected cortical regions projected, in part, to the same region of the caudate nucleus. In a later study, Selemon and Goldman-Rakic[53] found considerable overlap which was interdigitated, but not exclusively, in the ventromedial striatum. They were not able to assess the dorsolateral striatum. In a more recent study, Averbeck et al[11] using animal tract tracing in monkeys found that certain projection zone subregions, particularly, the medial rostral caudate nucleus of the striatum, received input from 5 separate prefrontal regions which they examined. We believe the above studies in monkeys clearly suggest that projection zone overlap is a characteristic feature of corticostriatal connectivity, although they do not provide a specific threshold for what might be considered a mixed or dominant voxel.

Despite the lack of biological certainty about an optimal threshold, we emphasize when we used the alternative thresholds of 0.5 and 0.9, we obtained similar results (see above, and supplementary figure S2). In fact, we do not believe there is any absolute threshold that divides mixed- vs dominant-input voxels. That is, we do not believe there are only 2 surface voxel projection zone subtypes; but, rather, that dividing striatal projection zones, based on cortical connectivity, into patterns of more integrative versus more dominant-input subtypes is a useful way to characterize brain wiring in this pathway.

In summary, using novel methods to assess frontostriatal structural connectivity, we show a less integrative pattern of frontostriatal structural connectivity in chronic schizophrenia, especially to LH limbic and associative striatum. Such aberrant brain wiring is consistent with a developmental model in schizophrenia, an idea we plan to investigate further by assessing these measures as potential biomarkers in larger samples in the early stage of the illness in schizophrenia.

Supplementary Material

Supplementary data are available at *Schizophrenia Bulletin* online.

Funding

VA Merit Awards CX000176 (M.E.S.); CX000157 (R.W.M.); R01 AG042512 (M.K.); R01 MH102377 (M.K.); RO3 MH110745 (A.E.L.); K01 MH115247-01A1 (A.E.L.); U01CA199459 (L.J.O.); P41EB015902; P41EB015898; R01MH074794; R01 MH119222 (Y.R.).

Conflict of Interest

None of the authors has conflicts of interest.

References

1. Alexander GE, Crutcher MD. Functional architecture of basal ganglia circuits: neural substrates of parallel processing. *Trends Neurosci*. 1990;13(7):266–271.
2. Alexander GE, DeLong MR, Strick PL. Parallel organization of functionally segregated circuits linking basal ganglia and cortex. *Annu Rev Neurosci*. 1986;9:357–381.
3. Manoach DS, Gollub RL, Benson ES, et al. Schizophrenic subjects show aberrant fMRI activation of dorsolateral prefrontal cortex and basal ganglia during working memory performance. *Biol Psychiatry*. 2000;48(2):99–109.
4. Voorn P, Vanderschuren LJ, Groenewegen HJ, Robbins TW, Pennartz CM. Putting a spin on the dorsal-ventral divide of the striatum. *Trends Neurosci*. 2004;27(8):468–474.
5. Bhatia KP, Marsden CD. The behavioural and motor consequences of focal lesions of the basal ganglia in man. *Brain*. 1994;117(Pt 4):859–876.
6. Calabresi P, De Murtas M, Bernardi G. The neostriatum beyond the motor function: experimental and clinical evidence. *Neuroscience*. 1997;78(1):39–60.
7. Cummings JL. Frontal-subcortical circuits and human behavior. *Arch Neurol*. 1993;50(8):873–880.
8. Levitt JJ, Kubicki M, Nestor PG, et al. A diffusion tensor imaging study of the anterior limb of the internal capsule in schizophrenia. *Psychiatry Res*. 2010;184(3):143–150.
9. Levitt JJ, McCarley RW, Dickey CC, et al. MRI study of caudate nucleus volume and its cognitive correlates in neuroleptic-naive patients with schizotypal personality disorder. *Am J Psychiatry*. 2002;159(7):1190–1197.
10. Levitt JJ, Nestor PG, Levin L, et al. Reduced structural connectivity in frontostriatal white matter tracts in the associative loop in schizophrenia. *Am J Psychiatry*. 2017;174(11):1102–1111.
11. Averbeck BB, Lehman J, Jacobson M, Haber SN. Estimates of projection overlap and zones of convergence within frontal-striatal circuits. *J Neurosci*. 2014;34(29):9497–9505.

12. Haber SN. The primate basal ganglia: parallel and integrative networks. *J Chem Neuroanat*. 2003;26(4):317–330.
13. Haber SN. Convergence of limbic, cognitive, and motor cortico-striatal circuits with dopamine pathways in primate brain. In: Iversen LL, Iversen SD, Dunnett SB, Bjorklund A, eds. *Dopamine Handbook*. Oxford: Oxford University Press, Inc.; 2010:38–48.
14. Draganski B, Kherif F, Klöppel S, et al. Evidence for segregated and integrative connectivity patterns in the human Basal Ganglia. *J Neurosci*. 2008;28(28):7143–7152.
15. Lehéricy S, Ducros M, Van de Moortele PF, et al. Diffusion tensor fiber tracking shows distinct corticostriatal circuits in humans. *Ann Neurol*. 2004;55(4):522–529.
16. Quan M, Lee SH, Kubicki M, et al. White matter tract abnormalities between rostral middle frontal gyrus, inferior frontal gyrus and striatum in first-episode schizophrenia. *Schizophr Res*. 2013;145(1–3):1–10.
17. First MB, Spitzer RL, Gibbon M, Williams JBW. *Structured Clinical Interview for DSM-IV Axis I Disorders - (SCID-I)*. Washington, DC: American Psychiatric Press; 1997.
18. First MB, Spitzer RL, Williams JBW, Gibbon M. *Structured Clinical Interview for DSM-IV - Non-Patient Edition (SCID-NP, version 1.0)*. Washington, DC: American Psychiatric Press; 1995.
19. Oldfield RC. The assessment and analysis of handedness: the Edinburgh inventory. *Neuropsychologia*. 1971;9(1):97–113.
20. Hollingshead A. *Two-Factor Index of Social Position*. New Haven, CT: Yale Station; 1965.
21. Fischl B, van der Kouwe A, Destrieux C, et al. Automatically parcellating the human cerebral cortex. *Cereb Cortex*. 2004;14(1):11–22.
22. Smith SM, Jenkinson M, Woolrich MW, et al. Advances in functional and structural MR image analysis and implementation as FSL. *Neuroimage*. 2004;23(suppl 1):S208–S219.
23. Levitt JJ, Rosow LK, Nestor PG, et al. A volumetric MRI study of limbic, associative and sensorimotor striatal subregions in schizophrenia. *Schizophr Res*. 2013;145(1–3):11–19.
24. Levitt JJ, Alvarado JL, Nestor PG, et al. Fractional anisotropy and radial diffusivity: diffusion measures of white matter abnormalities in the anterior limb of the internal capsule in schizophrenia. *Schizophr Res*. 2012;136(1–3):55–62.
25. Jenkinson M, Beckmann CF, Behrens TE, Woolrich MW, Smith SM. FSL. *Neuroimage*. 2012;62(2):782–790.
26. Ling J, Merideth F, Caprihan A, Pena A, Teshiba T, Mayer AR. Head injury or head motion? Assessment and quantification of motion artifacts in diffusion tensor imaging studies. *Hum Brain Mapp*. 2012;33(1):50–62.
27. Malcolm JG, Shenton ME, Rathi Y. Filtered multitensor tractography. *IEEE Trans Med Imaging*. 2010;29(9):1664–1675.
28. Rathi Y, Malcolm JG, Michailovich O, Westin CF, Shenton ME, Bouix S. Tensor kernels for simultaneous fiber model estimation and tractography. *Magn Reson Med*. 2010;64(1):138–148.
29. Fillard P, Descoteaux M, Goh A, et al. Quantitative evaluation of 10 tractography algorithms on a realistic diffusion MR phantom. *Neuroimage*. 2011;56(1):220–234.
30. Stoll AL. *The Psychopharmacology Reference Card*. Belmont, MA: McLean Hospital; 2009.
31. Woods SW. Chlorpromazine equivalent doses for the newer atypical antipsychotics. *J Clin Psychiatry*. 2003;64(6):663–667.
32. Kay SR, Fiszbein A, Opler LA. The positive and negative syndrome scale (PANSS) for schizophrenia. *Schizophr Bull*. 1987;13(2):261–276.
33. Haber SN. Neuroanatomy of reward: a view from the ventral striatum. In: Gottfried JA, ed. *Neurobiology of Sensation and Reward*. Boca Raton, FL: CRC Press; 2011.
34. Nambu A, Chiken S, Shashidharan P, et al. Reduced pallidal output causes dystonia. *Front Syst Neurosci*. 2011;5:89.
35. Murray RM, Lewis SW. Is schizophrenia a neurodevelopmental disorder? *Br Med J (Clin Res Ed)*. 1987;295(6600):681–682.
36. Weinberger DR. Implications of normal brain development for the pathogenesis of schizophrenia. *Arch Gen Psychiatry*. 1987;44(7):660–669.
37. Ripke S, Sanders AR, Kendler KS, et al. Genome-wide association study identifies five new schizophrenia loci. *Nature genetics*. 2011;43:969.
38. Sekar A, Bialas AR, de Rivera H, et al.; Schizophrenia Working Group of the Psychiatric Genomics Consortium. Schizophrenia risk from complex variation of complement component 4. *Nature*. 2016;530(7589):177–183.
39. Stephan AH, Barres BA, Stevens B. The complement system: an unexpected role in synaptic pruning during development and disease. *Annu Rev Neurosci*. 2012;35:369–389.
40. Wiegand LC, Warfield SK, Levitt JJ, et al. An in vivo MRI study of prefrontal cortical complexity in first-episode psychosis. *Am J Psychiatry*. 2005;162(1):65–70.
41. Palaniyappan L, Liddle PF. Aberrant cortical gyrification in schizophrenia: a surface-based morphometry study. *J Psychiatry Neurosci*. 2012;37(6):399–406.
42. Palaniyappan L, Mallikarjun P, Joseph V, White TP, Liddle PF. Folding of the prefrontal cortex in schizophrenia: regional differences in gyrification. *Biol Psychiatry*. 2011;69(10):974–979.
43. White T, Su S, Schmidt M, Kao CY, Sapiro G. The development of gyrification in childhood and adolescence. *Brain Cogn*. 2010;72:36–45.
44. Van Essen DC. A tension-based theory of morphogenesis and compact wiring in the central nervous system. *Nature*. 1997;385(6614):313–318.
45. Ono M, Kubik S, Abernathey CD. *Atlas of the Cerebral Sulci*. New York; Thieme Medical Publishers, Inc.; 1990.
46. Yücel M, Stuart GW, Maruff P, et al. Paracingulate morphologic differences in males with established schizophrenia: a magnetic resonance imaging morphometric study. *Biol Psychiatry*. 2002;52(1):15–23.
47. Nakamura M, Nestor PG, McCarley RW, et al. Altered orbitofrontal sulcogyral pattern in schizophrenia. *Brain*. 2007;130(pt 3):693–707.
48. Haber SN, Fudge JL, McFarland NR. Striatonigrostriatal pathways in primates form an ascending spiral from the shell to the dorsolateral striatum. *J Neurosci*. 2000;20(6):2369–2382.
49. Crow TJ, Paez P, Chance SA. Callosal misconnectivity and the sex difference in psychosis. *Int Rev Psychiatry*. 2007;19(4):449–457.
50. Savadjiev P, Seidman LJ, Thermenos H, et al. Sexual dimorphic abnormalities in white matter geometry common to

schizophrenia and non-psychotic high-risk subjects: evidence for a neurodevelopmental risk marker? *Hum Brain Mapp*. 2016;37(1):254–261.

51. Cullen TJ, Walker MA, Eastwood SL, Esiri MM, Harrison PJ, Crow TJ. Anomalies of asymmetry of pyramidal cell density and structure in dorsolateral prefrontal cortex in schizophrenia. *Br J Psychiatry*. 2006;188:26–31.
52. Yeterian EH, Van Hoesen GW. Cortico-striate projections in the rhesus monkey: the organization of certain cortico-caudate connections. *Brain Res*. 1978;139(1): 43–63.
53. Selemon LD, Goldman-Rakic PS. Longitudinal topography and interdigitation of corticostriatal projections in the rhesus monkey. *J Neurosci*. 1985;5(3):776–794.